The workshop on partial differential equations on the sphere 2019
Agora Hydro-Québec, Pavilion Cœur des Sciences, UQÀM, Montréal, Québec, Canada
1 May 2019

Application of spherical helix nodes to a shallow-water model using radial basis functions

Takeshi Enomoto @takeshi_enomoto
Disaster Prevention Research Laboratory
Kyoto University

Supported by JSPS KAKENHI Grant Number 15K13417 and
by MEXT as “Exploratory Challenge on Post-K computer”
(Elucidation of the Birth of Exoplanets [Second Earth] and
the Environmental Variations of Planets in the Solar System)

Pole problem

- Severe limitation of time-step due to the small zonal interval near the pole with lat-lon grid, calling for quasi-uniform distribution

- However, no obvious methods known to distribute many points uniformly on the sphere

- One of 18 mathematical problems left for 21C (Smale 1998)

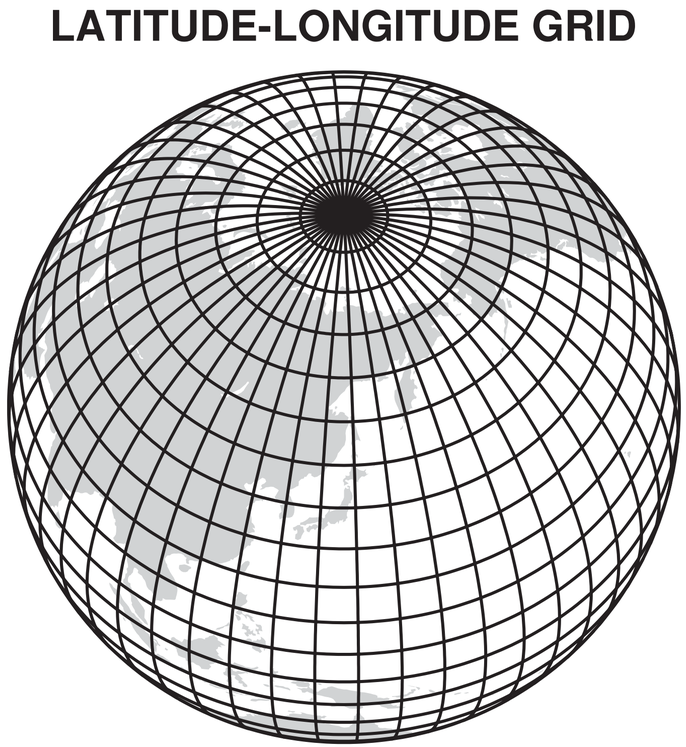

Williamson 2007

Quasi-uniform nodes on the sphere

ME: Minimum Energy

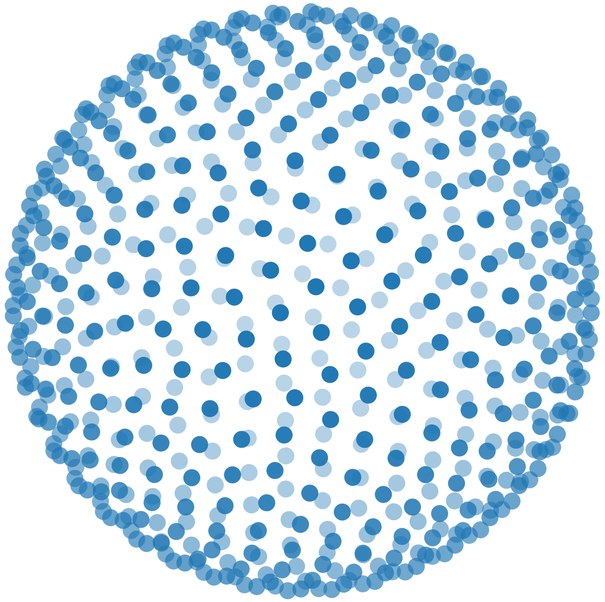

https://github.com/gradywright/spherepts

SH: Spherical Helix

$\lambda = m\theta \mod 2\pi$

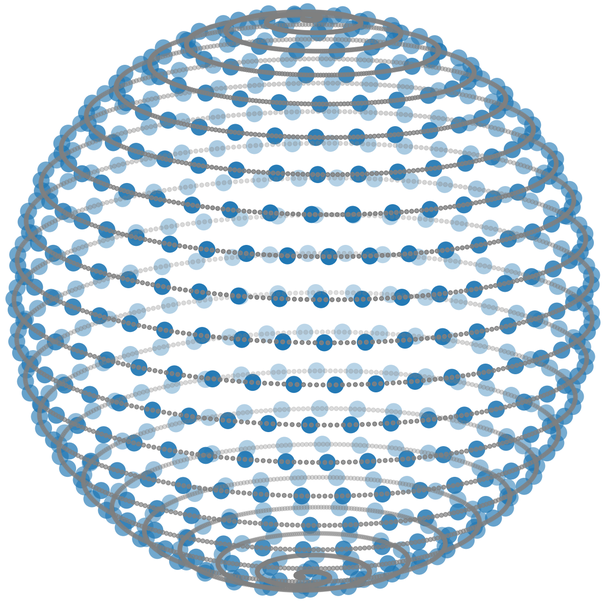

Bauer 2000

NI: Icosahedral NICAM

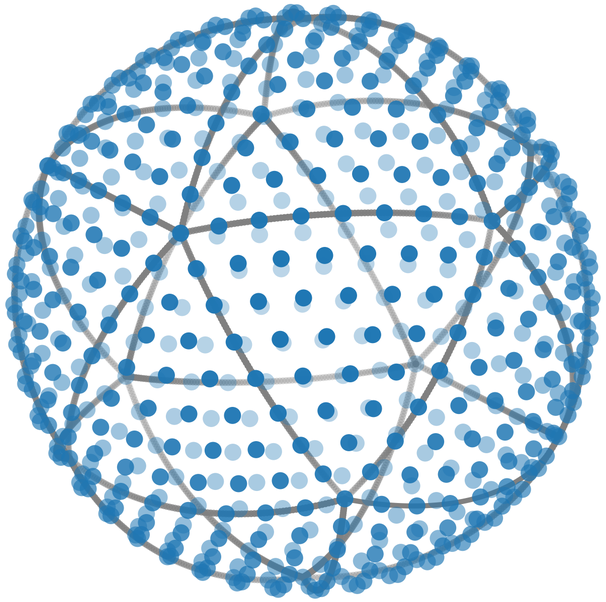

Tomita et al. 2001

Spherical Helix

- Helix equation $\lambda = m\theta \bmod 2\pi$
- Assume equal interval and pitch to obtain
  $\Delta s \approx 2m/n$
  $\Delta\theta = 2\pi/m$
  $m = \sqrt{n\pi}$ (Bauer 2000)
- For almost constant intervals $\cos\theta_k = 1 - \dfrac{2k-1}{n}$
- No iteration
- No limitation on the number of nodes

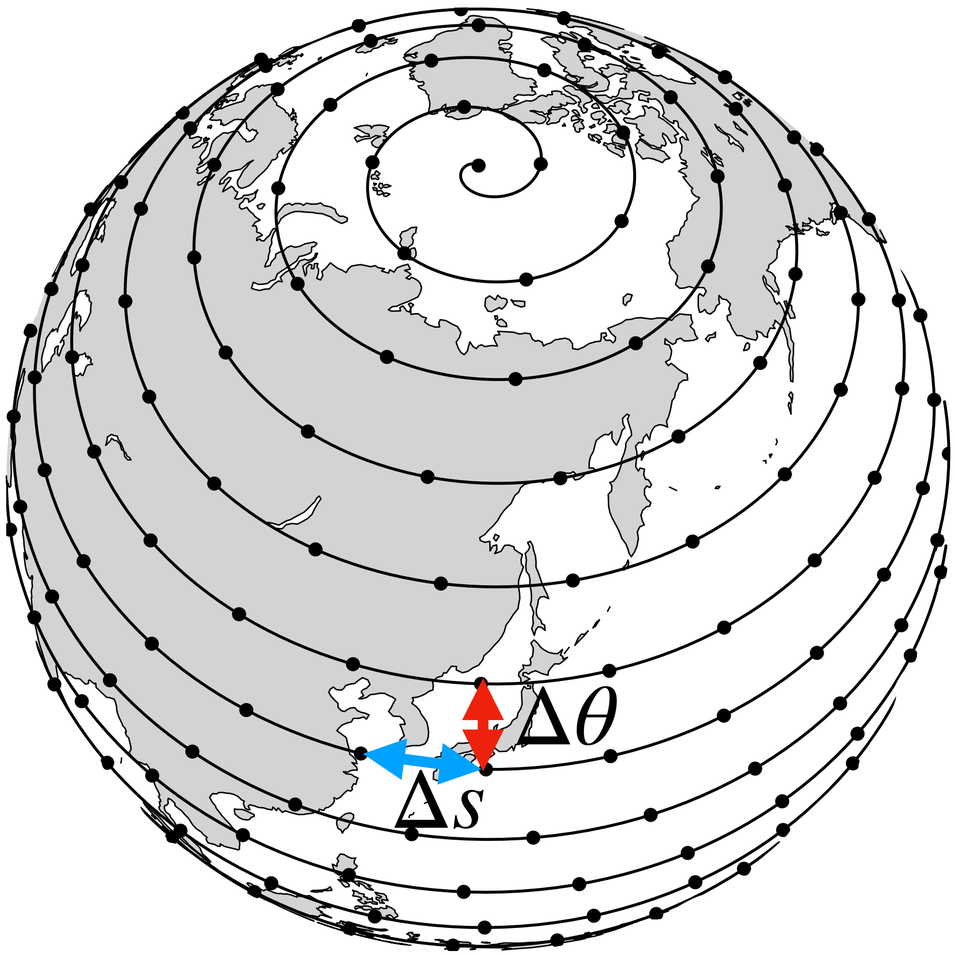

Application of RBF to PDES

- Advection on the sphere: Flyer and Wright (2007)
- Shallow water equations: Flyer and Wright (2009)
- Mesh-free: no staggering, irregular geometry, local refinement
- Quasi-uniform nodes for a longer time step
- Spectral convergence with a very simple algorithm
- Locality: less aliasing and Gibbs phenomena (Fornberg et al. 2008)

RBF: Radial Basis Functions

- RBF depends on the distance *r* from the node
- Shape parameter ε determines the radius of influence

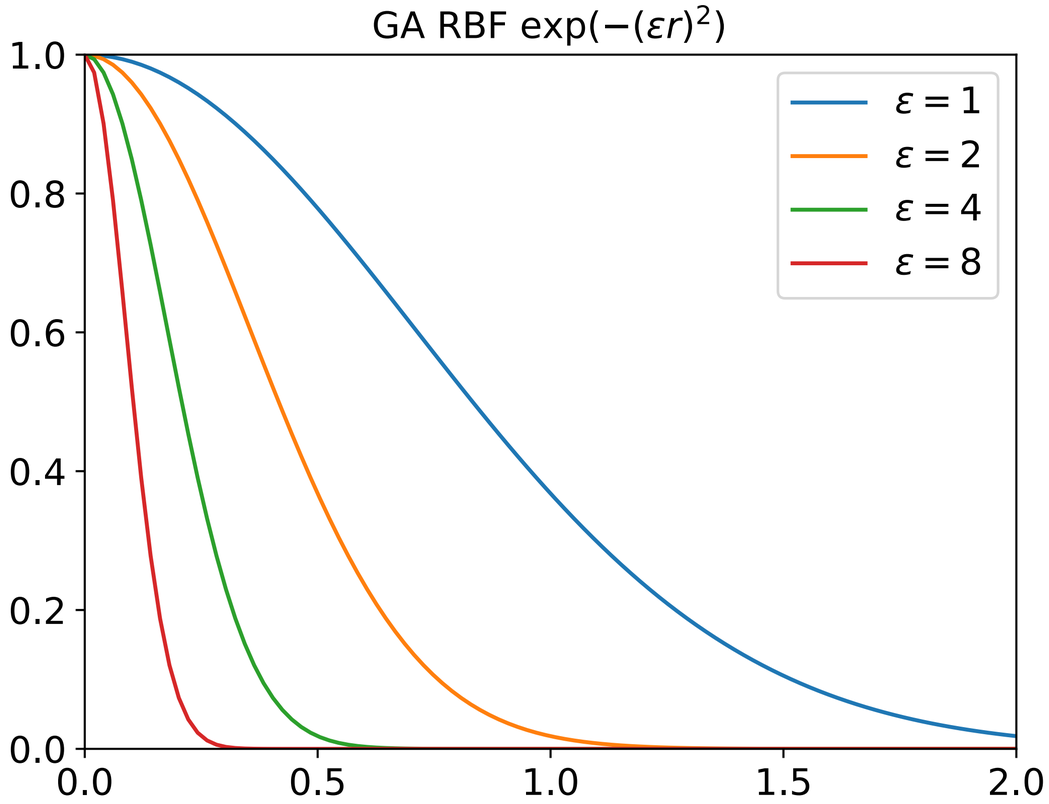

Type of RBF

- Infinitely smooth: GA, MQ, etc

$$\frac{\mathrm{d}}{\mathrm{d}r}\sqrt{1+(\varepsilon r)^2} = \frac{\varepsilon^2 r}{\sqrt{1+(\varepsilon r)^2}}$$

$$\frac{\mathrm{d}}{\mathrm{d}r}\exp\left[-(\varepsilon r)^2\right] = -2\varepsilon^2 r \exp\left[-(\varepsilon r)^2\right]$$

- Piecewise smooth: cubic, thin plate spline

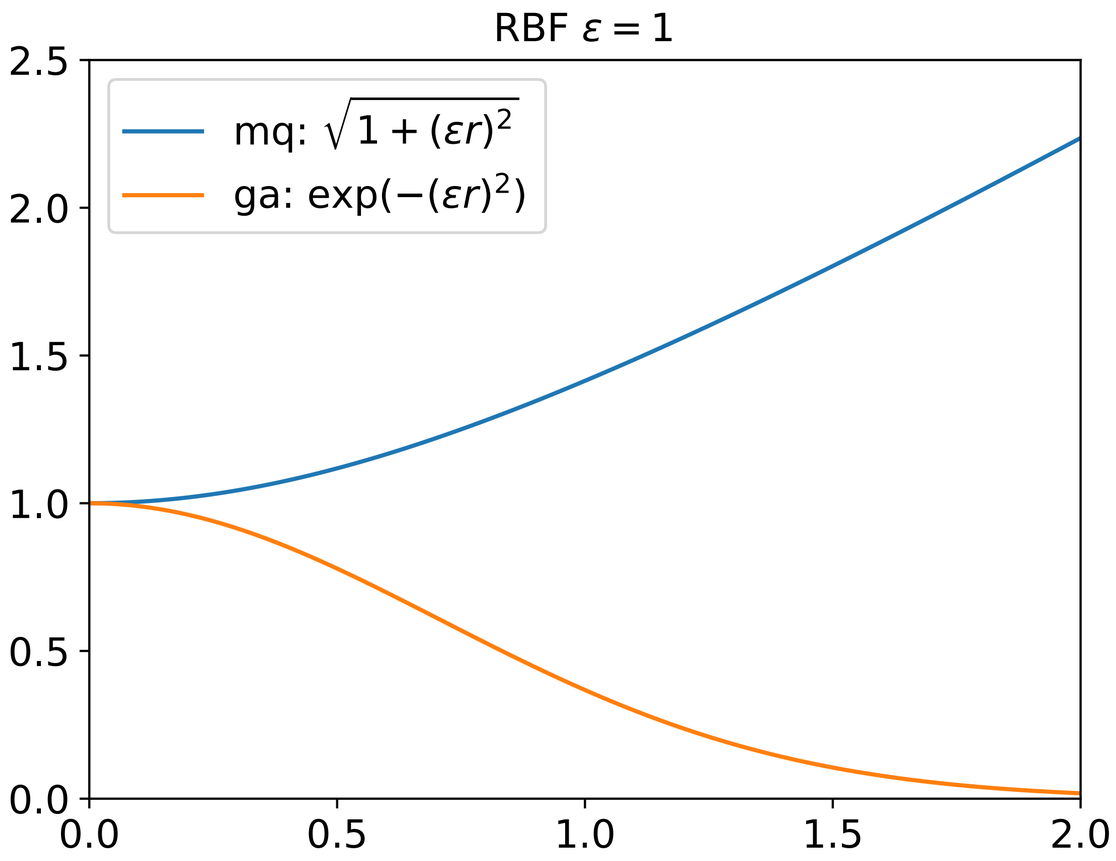

RBF Interpolation

RBF expansion $$f\left(\underline{x}\right) \approx s\left(\underline{x}\right) = \sum_{k=1}^{n} c_k \phi\left(r_k\right) \qquad r_k = \left\| \underline{x} - \underline{x}_k \right\|$$

Data and nodes $$\mathbf{f} \equiv \left[f_1, f_2, \cdots f_n\right]^{\mathsf{T}} \quad f_k = f\left(\underline{x}_k\right)$$

Collocation condition $$\mathbf{f} = \mathsf{A}\mathbf{c} \qquad \mathbf{c} \equiv \left[c_1, c_2, \cdots c_n\right]^{\mathsf{T}}$$

$$\mathsf{A} \equiv \begin{bmatrix} \phi(0) & \phi(r_{1,2}) & \cdots & \phi(r_{1,n}) \\ \phi(r_{2,1}) & \phi(0) & \cdots & \phi(r_{2,n}) \\ \vdots & \vdots & \ddots & \vdots \\ \phi(r_{n,1}) & \phi(r_{n,2}) & \cdots & \phi(0) \end{bmatrix} \qquad r_{i,j} \equiv = \left\| \underline{x}_i - \underline{x}_j \right\|$$

Nodal weight

- Surface of a unit sphere 4π
- uniform weight of a node $4\pi/n$
- Sums of each column of RBF interpolation matrix

$$\mathbf{w} = 4\pi \frac{\mathsf{A}^{-1}\mathbf{e}}{\mathbf{e}^{\mathsf{T}}\mathsf{A}^{-1}\mathbf{e}}$$

$$\mathbf{e} \equiv [1,1,\cdots,1]^{\mathsf{T}}$$

Sommariva and Vianello 2005

Error from uniform weight $4\pi/n$

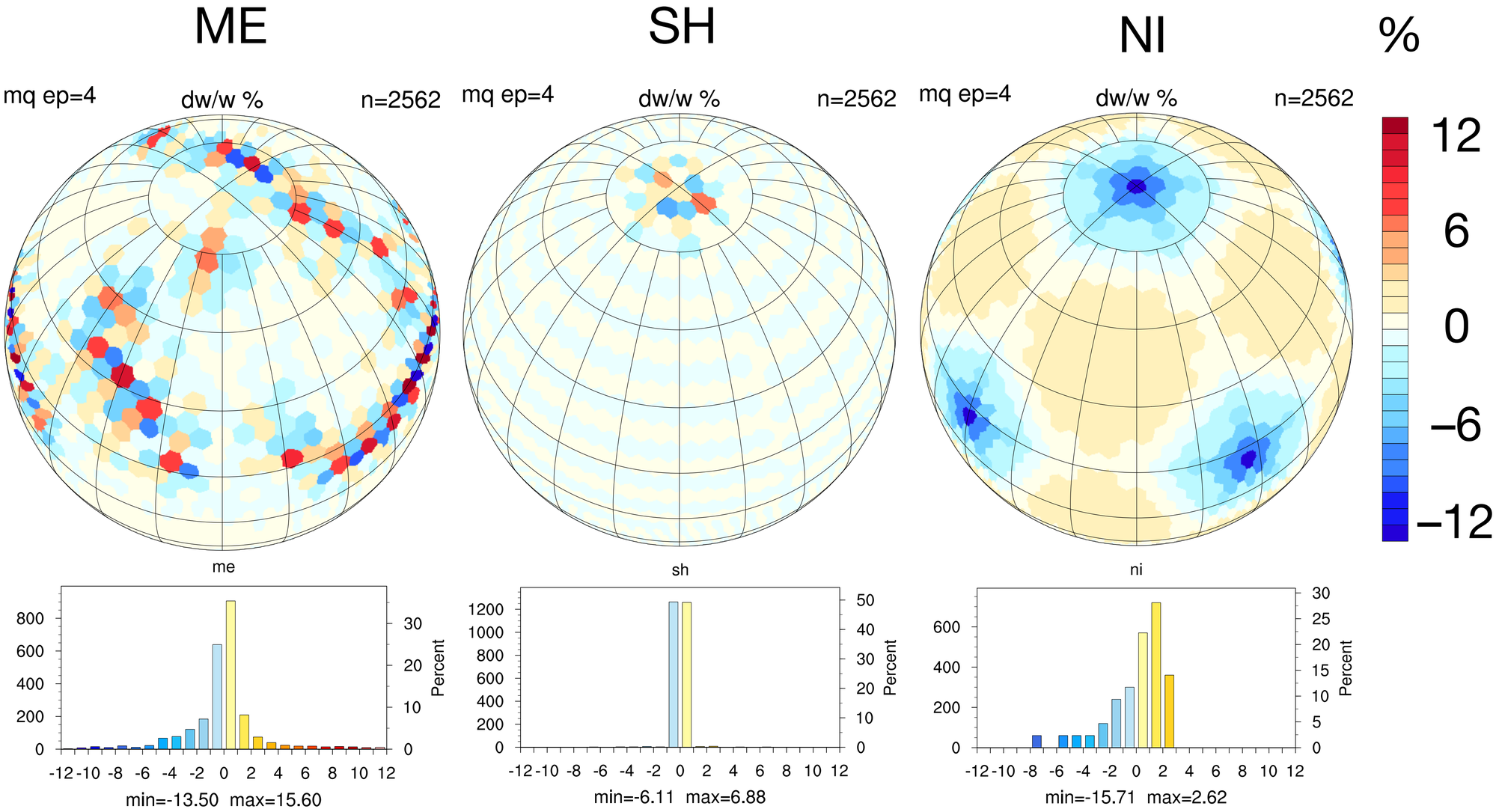

Derivative operator

Distance $$r_k(\underline{x}) = \left\| \underline{x} - \underline{x}_k \right\| = \sqrt{(x - x_k)^2 + (y - y_k)^2 + (z - z_k)^2}$$

Differentiate RBF $$\nabla f\left(\underline{x}\right) \approx \nabla \left[\sum_{k=1}^{n} c_k \phi\left(r_k\left(\underline{x}\right)\right) \right] = \sum_{k=1}^{n} c_k \nabla \phi\left(r_k\left(\underline{x}\right)\right)$$

Gradient of RBF $$\nabla \phi\left(r_k\left(\underline{x}\right)\right) = \frac{\mathrm{d}\phi\left(r_k\left(\underline{x}\right)\right)}{\mathrm{d}r} \nabla r_k\left(\underline{x}\right) = \phi'\left(r_k\left(\underline{x}\right)\right) \frac{\underline{x} - \underline{x}_k}{r_k\left(\underline{x}\right)}$$

Flyer and Wright 2009

Shallow water model

Cartesian formulation

$$\frac{\partial \underline{u}}{\partial t} = -\left(\underline{u} \cdot P\nabla\right)\underline{u} - f\left(\underline{x} \times \underline{u}\right) - g\nabla h + \mu \underline{x}$$

$$\frac{\partial h}{\partial t} = -\nabla \cdot (h\underline{u})$$

$P \equiv I - \underline{x}\underline{x}^{\mathrm{T}}$ projects a vector to the tangent plane

$\mu = \underline{x} \cdot \left\{\left(\underline{u} \cdot P\nabla\right)\underline{u}\right\}$ Lagrange multiplier (Côté 1988)

Flyer and Wright 2009

Projection to the tangent plane

radial component $\underline{x}\underline{x}^\top \underline{u}$ tangential component $\underline{u} - \underline{x}\underline{x}^\top \underline{u}$

$$P = I - \underline{x}\underline{x}^\top = \begin{bmatrix} 1 - x^2 & -xy & -xz \\ -xy & 1 - y^2 & -yz \\ -xz & -yz & 1 - z \end{bmatrix}$$

$$P \nabla \phi \left(r_k \left(\underline{x} \right) \right) = \begin{bmatrix} x\underline{x}^\top \underline{x}_k - x_k \\ y\underline{x}^\top \underline{x}_k - y_k \\ z\underline{x}^\top \underline{x}_k - z_k \end{bmatrix} \frac{\phi' \left(r_k \left(\underline{x} \right) \right)}{r_k \left(\underline{x} \right)}$$

Derivative matrix

$$P \nabla \mathbf{f} \Big|_x = (\mathsf{B}^x \mathsf{A}^{-1}) \mathbf{f}$$

$$\mathsf{B}^k_{j,k} \equiv \left[x_j \underline{x}_j \underline{x}_k^\mathsf{T} - x_k \right] \frac{\phi'\left(r_{j,k}\right)}{r_{j,k}}$$

Solve the linear system for D^x

$$\mathsf{D}^x \mathsf{A} = \mathsf{B}^x$$

Similarly, D^y and D^z are obtained.

Numerical studies

- Standard test for shallow water equations (Williamson et al. 1992)
  - Seven tests including steady-state, flow over isolated mountain, and Rossby-Haurwitz wave
  - RBF filter (Fornberg and Lehto 2011) as numerical diffusion in Case 5–7
- 4th Runge-Kutta for time integration
- Compare ME, NI, and SH with 2562 nodes (g-level 4)∼T51

Case 3: Geostrophic flow with compact support

$$n = 2562; \Delta t = 24\,\mathrm{min}\ \varepsilon = 4.75$$

ME

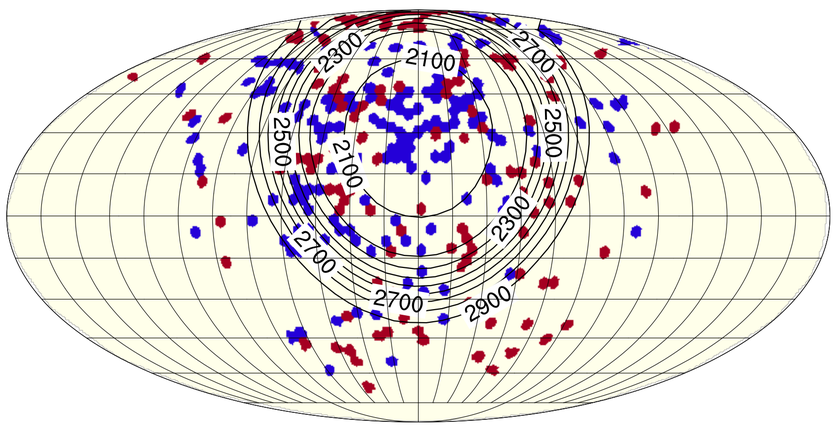

SH

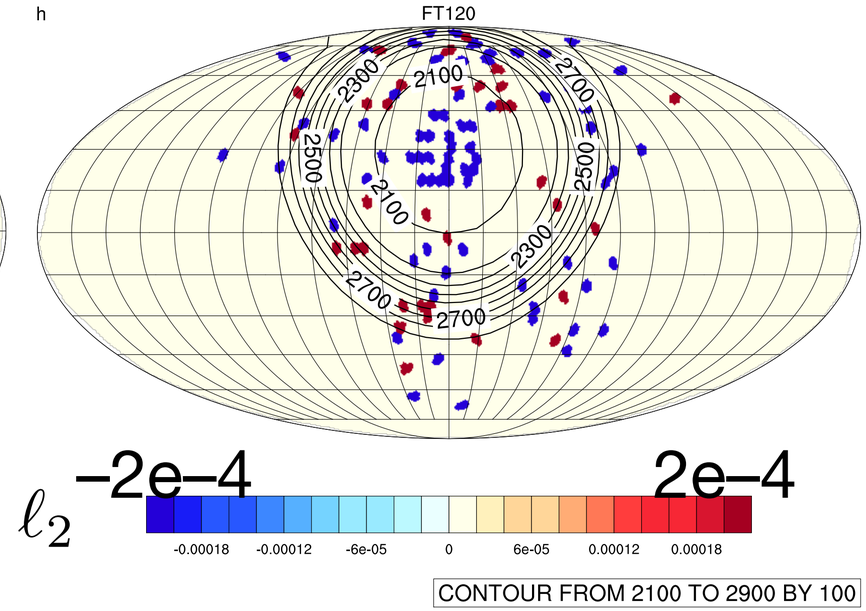

NI

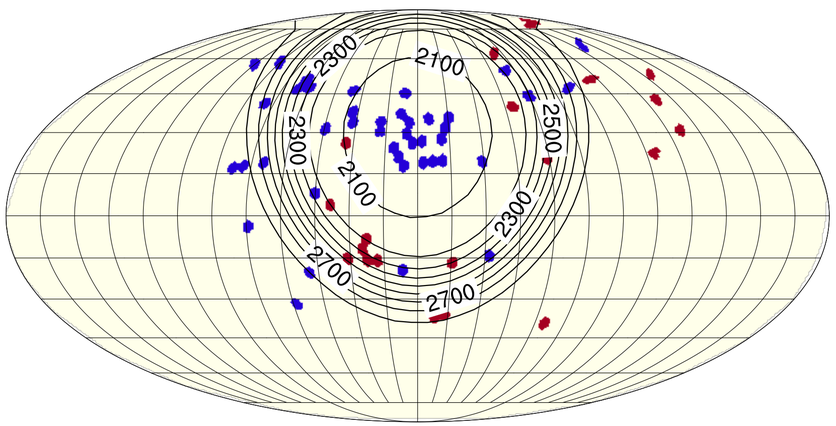

Case 3: Geostrophic flow with compact support

$$n = 2562; \Delta t = 24\,\mathrm{min}\ \varepsilon = 4.75$$

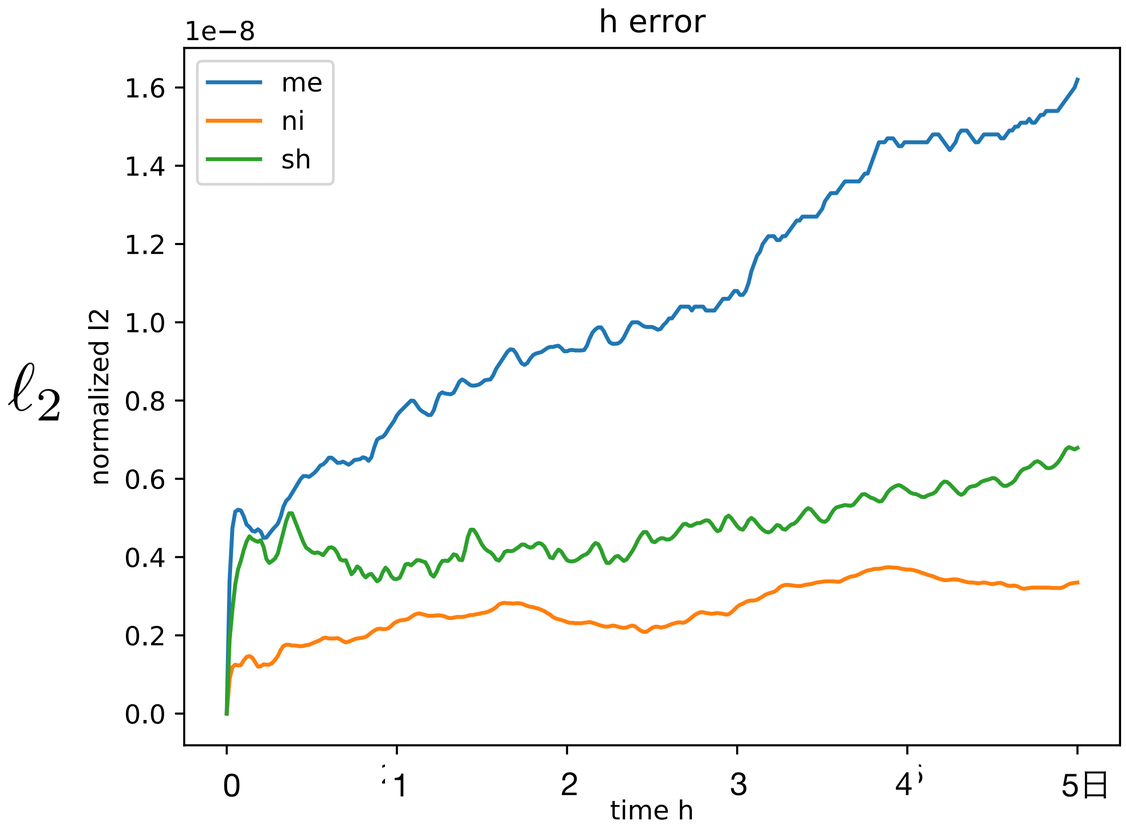

ℓ_2

Time

ME 1.62×10⁻⁸

SH 0.679×10⁻⁸

NI 0.335×10⁻⁸

Tomita et al. 2004	2562		1×10^{-3}
method	no. of nodes (N)	time step (Δt)	relative ℓ_2 error in h
RBF leapfrog	784 (28)	20 min	6.32×10^{-6}
	1849 (43)	12 min	1.97×10^{-8}
Flyer and Wright 2009	3136 (56)	10 min	3.65×10^{-10}
	4096 (64)	8 min	4.72×10^{-11}
Spherical Harmonics	5041 (71)	6 min	6.88×10^{-12}
SH; Jakob-Chien *et al.* (1995)	8192 (1849)	20 min* (3)	7×10^{-10}
Double Fourier	18 432 (4096)	15 min*	2.5×10^{-10}
DF/SHF; Spotz *et al.* (1998)	2048	6 min	2×10^{-6}
	8192	3 min	4×10^{-10}
Spectral Element	32 768	90 s	2×10^{-13}
SE; Taylor *et al.* (1997)	6144	90 s	8×10^{-7}
	24 576	45 s	1×10^{-10}
RBF SH RK4	2562 (51)	24 min	6.79×10^{-9}

*Semi-implicit

RBF hyperviscosity

Fornberg and Lehto 2011

- A^{-1} damps low order eigenfunctions weakly and high order eigenfunctions extremely fast.
- Irrespective of node distribution, number of dimensions, type of RBF.
- No decision required for what power of the Laplacian.
- No ode can grow for any ε

Case 5: Flow over an isolated mountain

$$n = 2562 \; \Delta t = 15\,\mathrm{min} \; \varepsilon = 4.25 \; \gamma = -2 \times 10^{-8}$$

ME

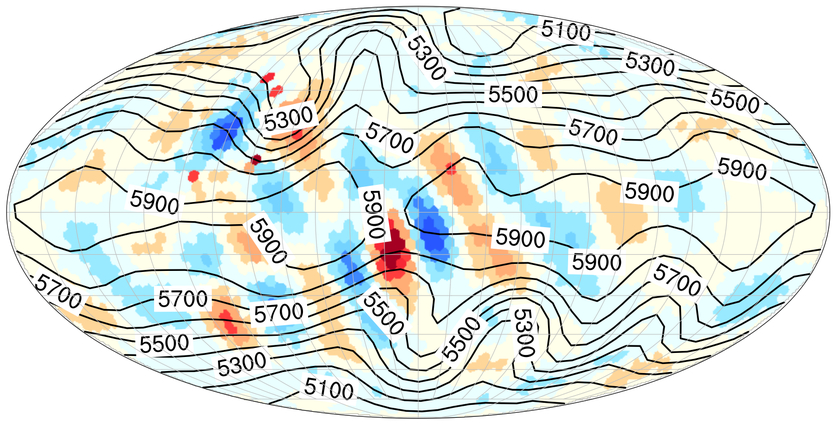

SH

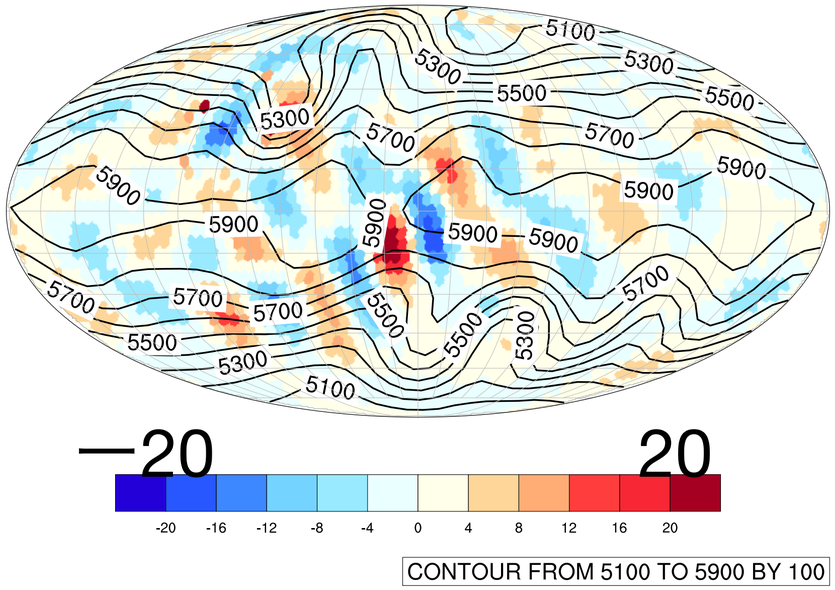

NI

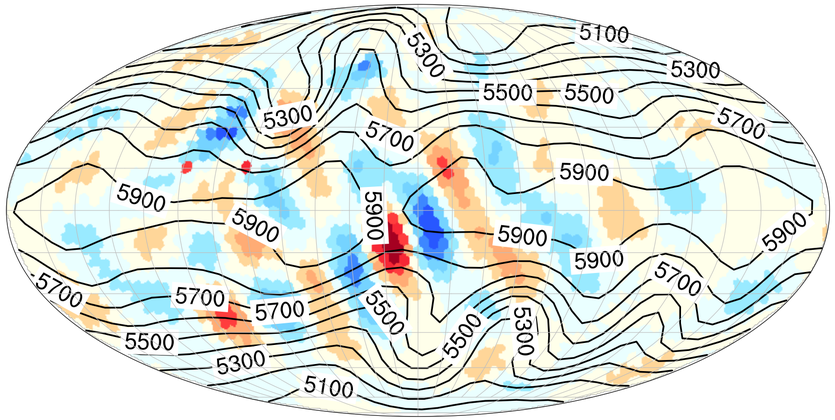

Case 5: Flow over an isolated mountain

$$n = 2562 \; \Delta t = 15\,\mathrm{min} \; \varepsilon = 4.25 \; \gamma = -2 \times 10^{-8}$$

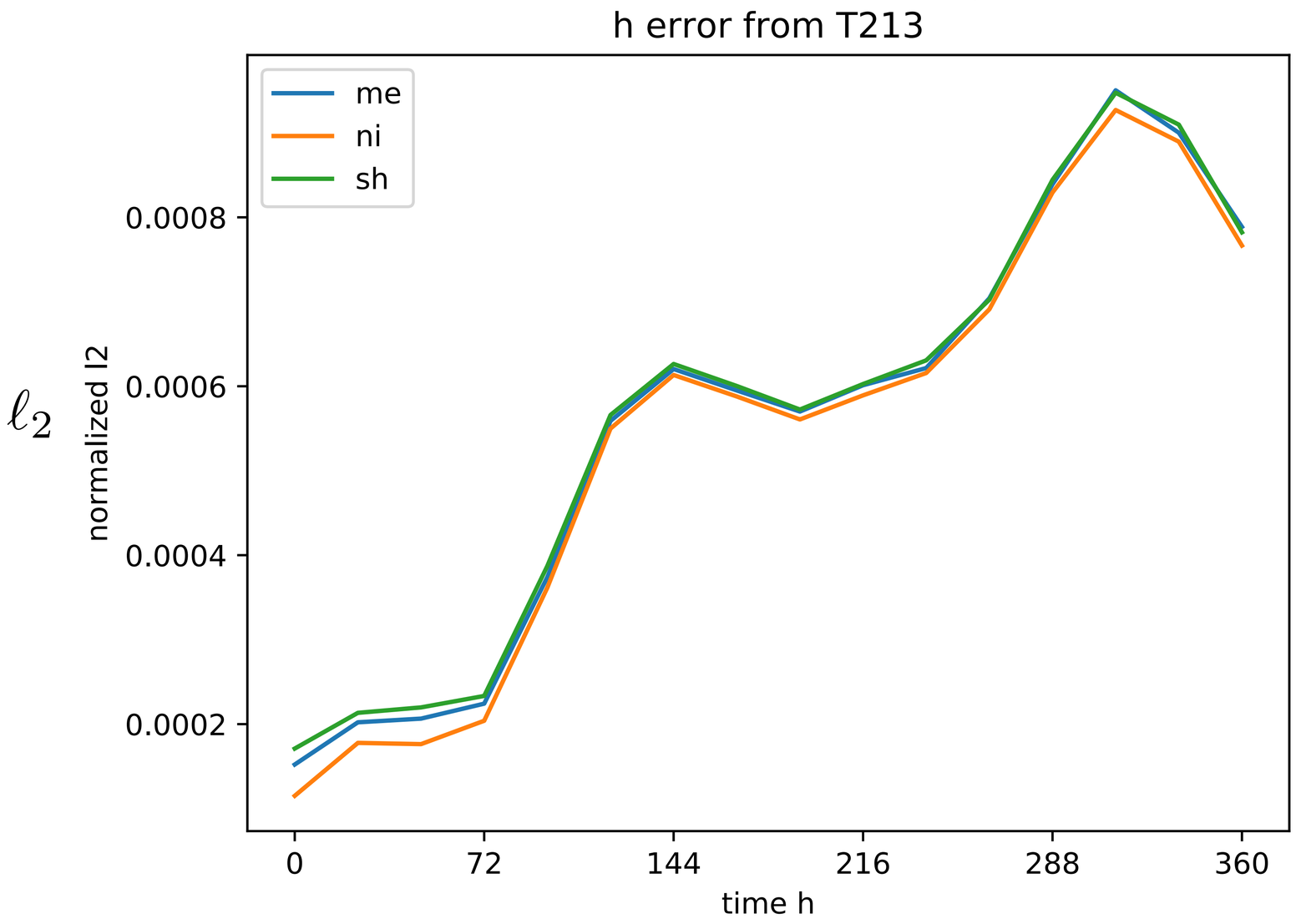

ME 7.89x10^{-4}

SH 7.67×10^{-4}

NI 7.82×10^{-4}

Case 5: Flow over an isolated mountain

$$n = 2562 \; \Delta t = 15\,\mathrm{min} \; \varepsilon = 4.25 \; \gamma = -2 \times 10^{-8}$$

mass

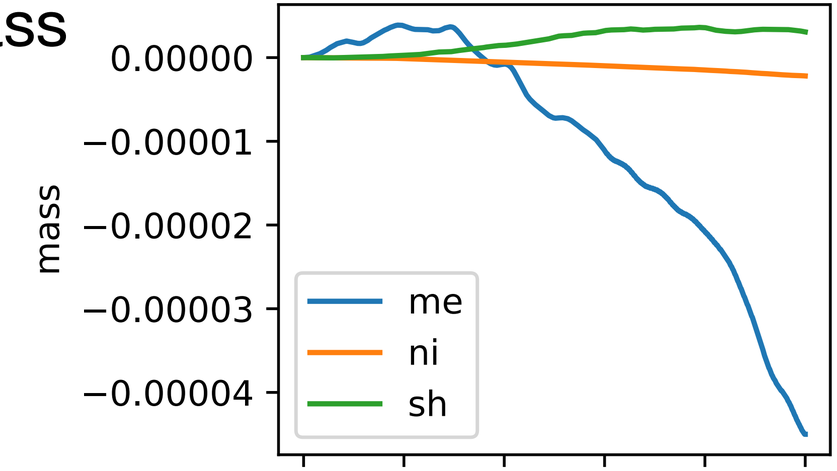

vorticity

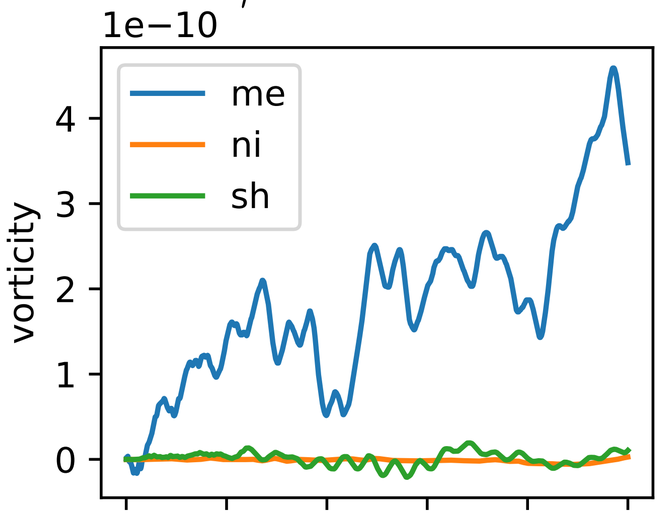

energy

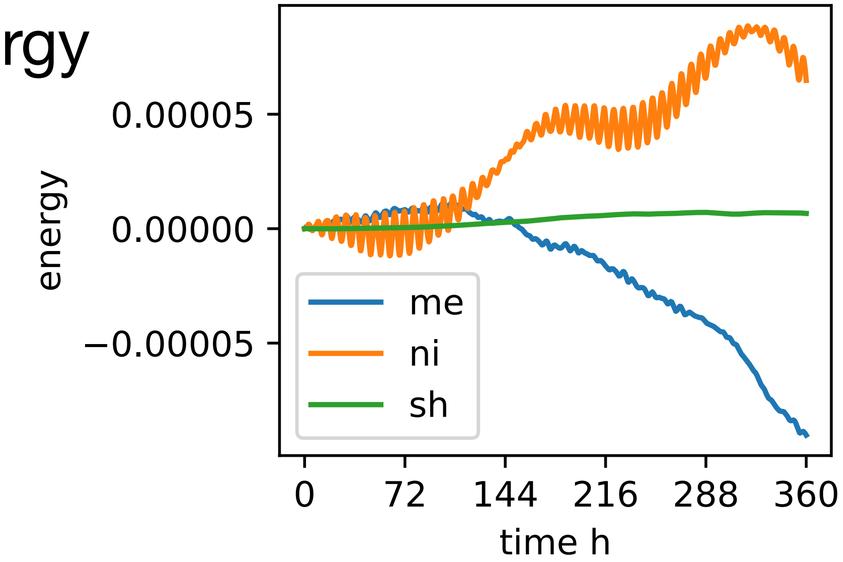

divergence

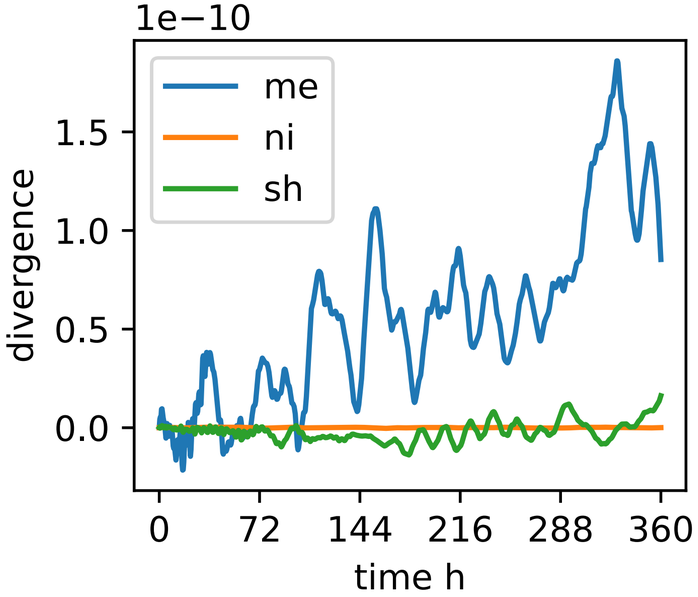

Case 7: Forecast from 500 hPa analysis

$$n = 2562 \; \Delta t = 15\,\mathrm{min} \; \varepsilon = 4.25 \; \gamma = -2 \times 10^{-7} \qquad t = 5 \text{ 日}$$

ME

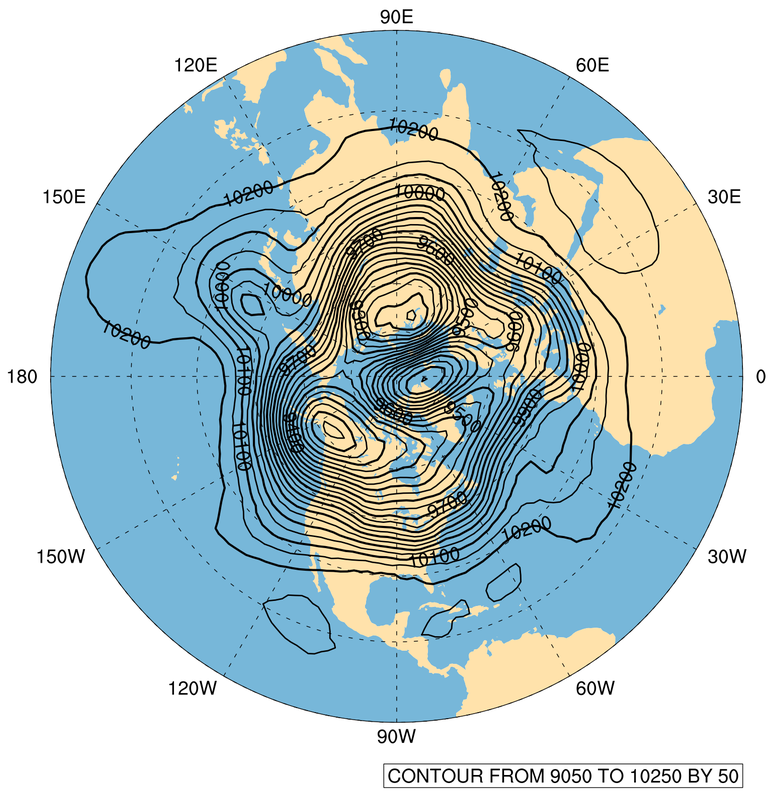

SH

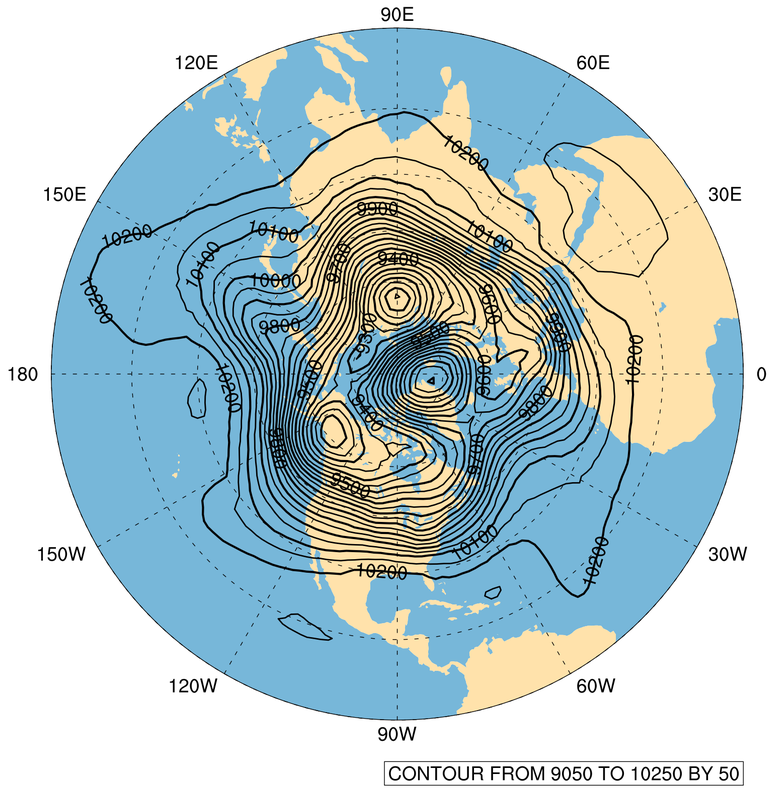

NI

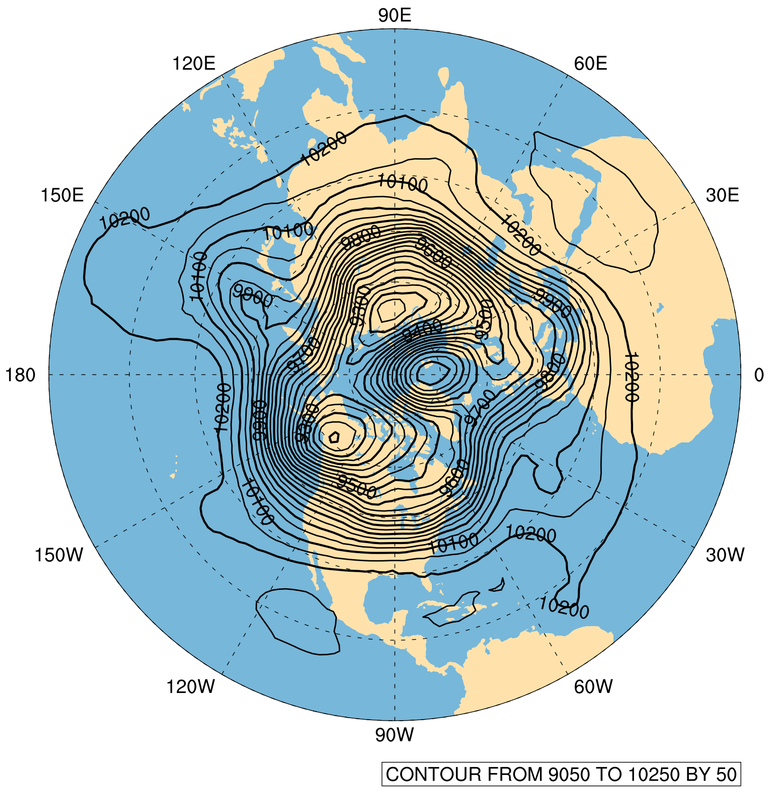

Case 7: Forecast from 500 hPa analysis

Error from reference T213 (contours)

>30N

ME

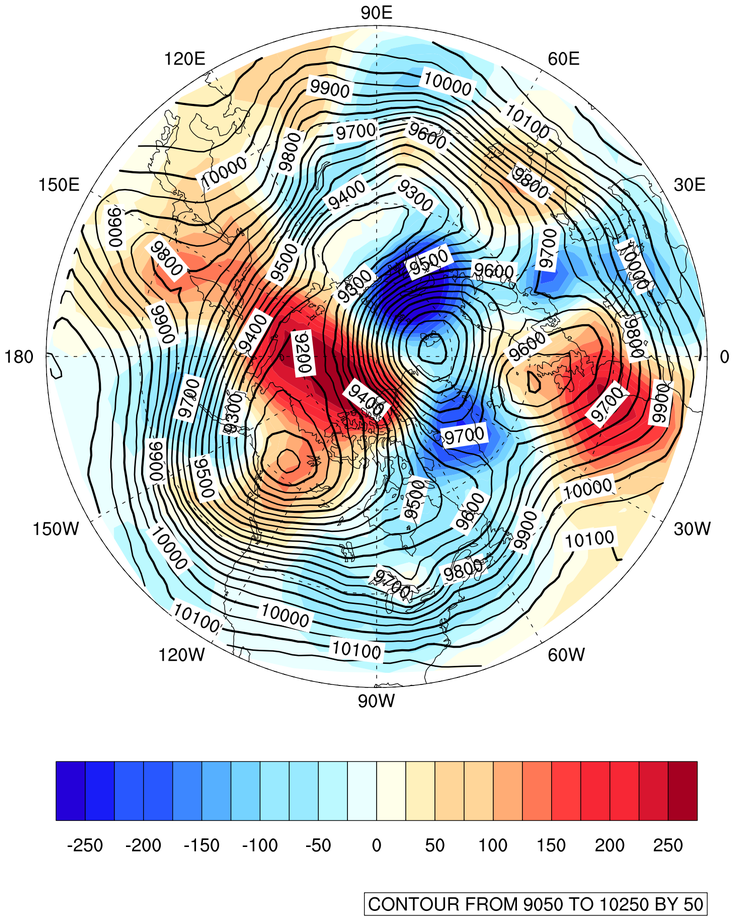

SH

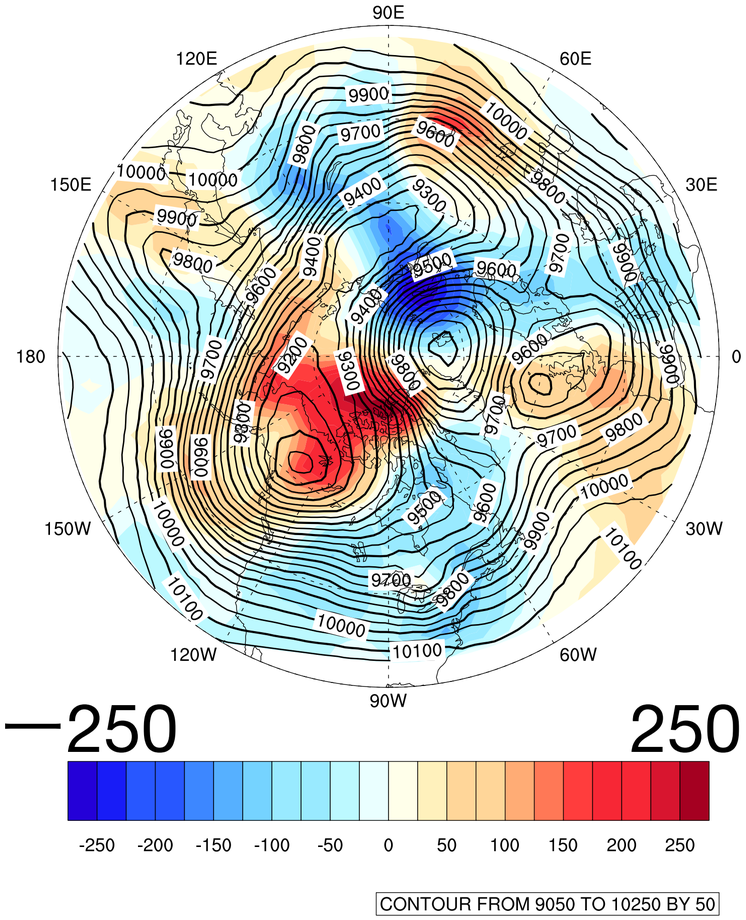

NI

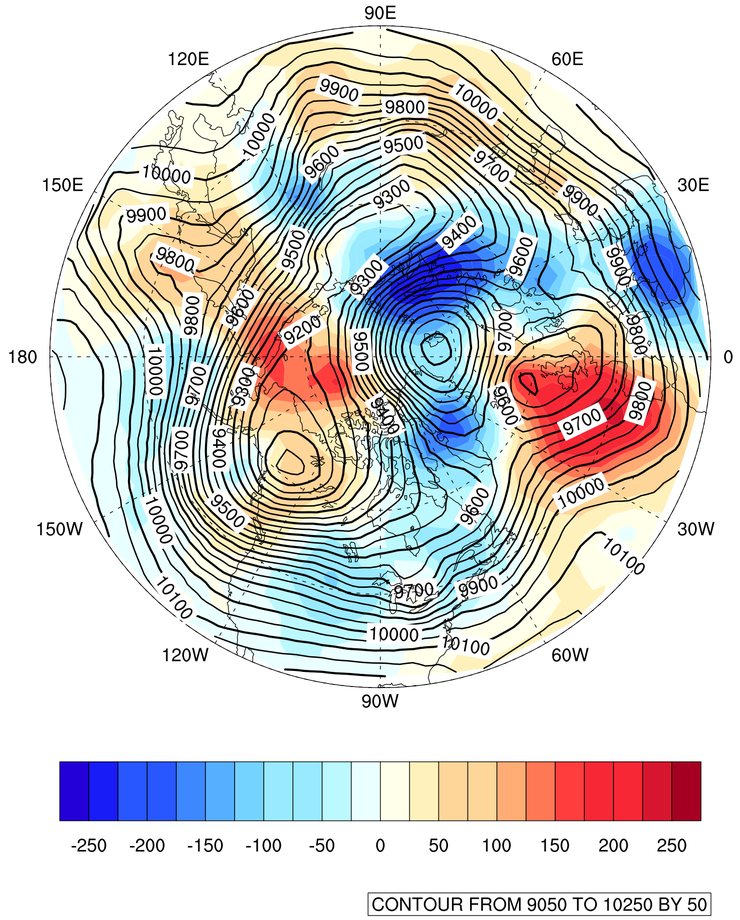

—250 250

Case 7: Forecast from 500 hPa analysis

$$n = 2562 \; \Delta t = 15\,\mathrm{min} \; \varepsilon = 4.25 \; \gamma = -2 \times 10^{-7}$$

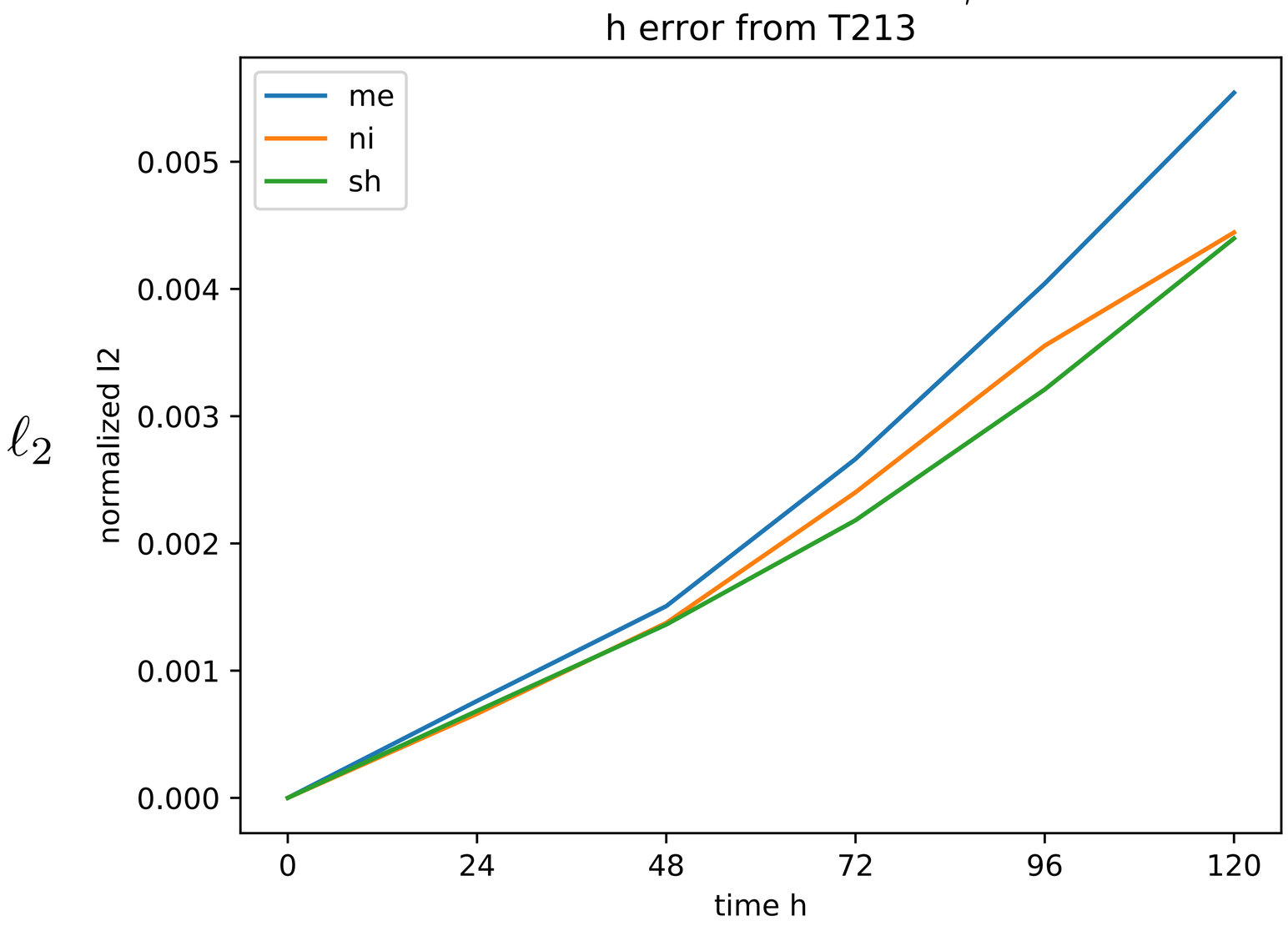

ME 5.54×10^{-3}

NI 4.44×10^{-3}

SH 4.40×10^{-3}

Case 7: Forecast from 500 hPa analysis

$$n = 2562 \; \Delta t = 15\,\mathrm{min} \; \varepsilon = 4.25 \; \gamma = -2 \times 10^{-7}$$

mass

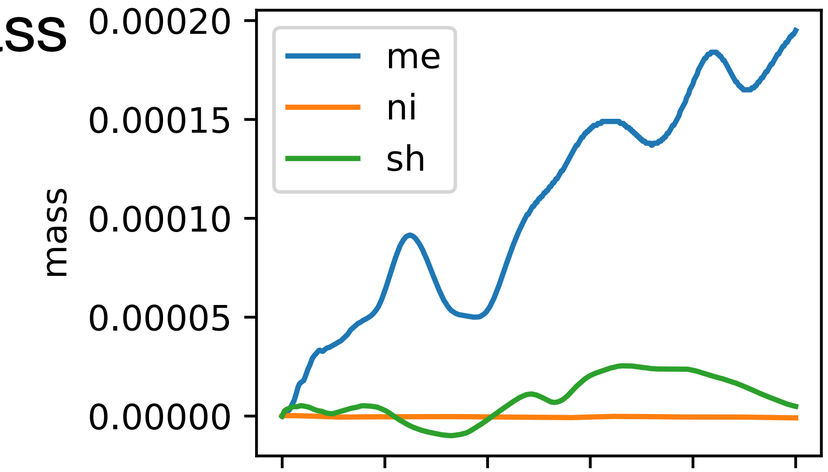

vorticity

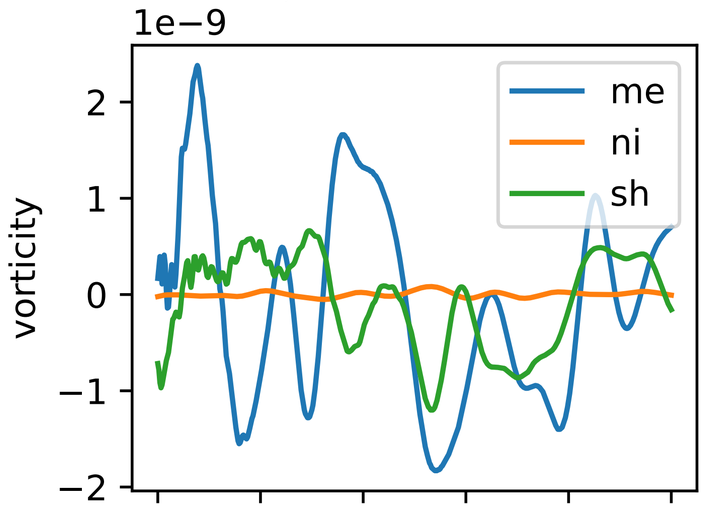

energy

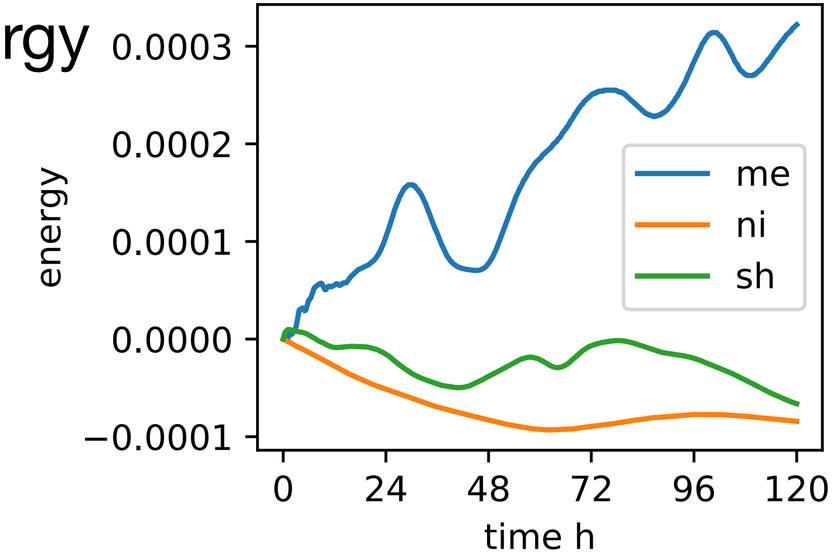

divergence

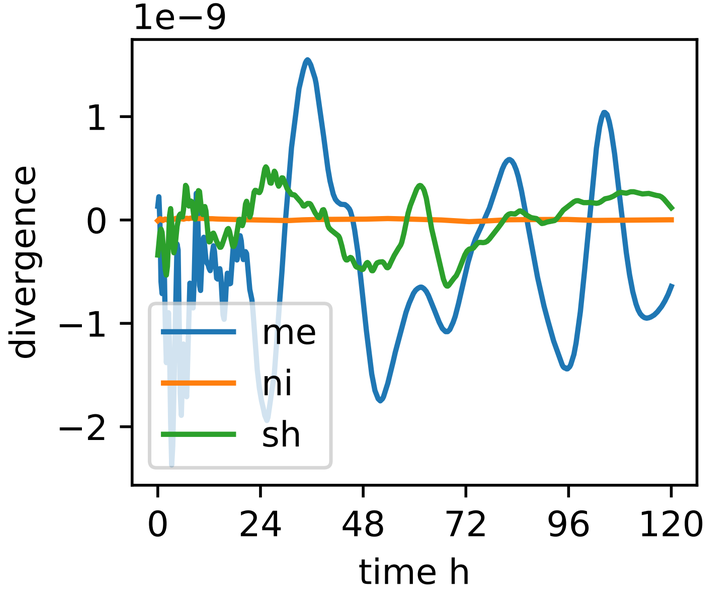

Settings and l2 norms

case	2	3	5	6	7
Δt m	24			15	
ε	4.75		4	4.25	
γ	NA		–2E-08	–2E-7	
NI	2.15E-09	3.35E-09	7.67E-04	6.05E-03	4.44E-03
ME	5.39E-09	1.62E-08	7.89E-04	6.81E-03	5.54E-03
SH	7.91E-10	6.79E-09	7.82E-04	8.01E-03	4.40E-03

Summary

- Minimum Energy: “Scars”, Spherical Helix: Poles, Icosahedron: Vertices
- In steady state tests, RBF is not as robust as the spectral method but very accurate.
- Spherical helix and NICAM nodes are better than minimum energy nodes, but the differences are less significant in realistic tests.
- NICAM nodes have a good conservation of vorticity and divergence.

Q&A

Q. Subich: What are possible causes of the differences in time evolution of error in conservation?

A. It may be related to the inhomogeneity such as scars in ME.

Q. Behrens: Have you tested other RBF?

A. GA seems to be more sensitive to the shape parameter than ME.

Q. Côte: What is the computational complexity?

A. O(n3) to solve linear systems in precomputation and O(n2) matrix operations per time step. Techniques exist to reduce computational loads.